Resolving voltage-dependent structural changes of a membrane photoreceptor by surface-enhanced IR difference spectroscopy

X. Jiang*[†], E. Zaitseva[†‡], M. Schmidt[‡], F. Siebert[‡], M. Engelhard[§], R. Schlesinger[¶], K. Ataka*, R. Vogel[‡‖], and J. Heberle*[‖]

*Department of Biophysical Chemistry (PC III), Bielefeld University, 33615 Bielefeld, Germany; [‡]Institute of Molecular Medicine and Cell Research, AG Biophysics, Albert-Ludwigs-Universität Freiburg, 79104 Freiburg, Germany; [§]Max Planck Institute of Molecular Physiology, D-44221 Dortmund, Germany; and [¶]Research Center Jülich, Institute of Neuroscience and Biophysics (INB-2), 52425 Jülich, Germany

Edited by Peter Brzezinski, Stockholm University, Stockholm, Sweden, and accepted by the Editorial Board June 27, 2008 (received for review March 6, 2008)

Membrane proteins are molecular machines that transport ions, solutes, or information across the cell membrane. Electrophysiological techniques have unraveled many functional aspects of ion channels but suffer from the lack of structural sensitivity. Here, we present spectroelectrochemical data on vibrational changes of membrane proteins derived from a single monolayer. For the seven-helical transmembrane protein sensory rhodopsin II, structural changes of the protein backbone and the retinal cofactor as well as single ion transfer events are resolved by surface-enhanced IR difference absorption spectroscopy (SEIDAS). Angular changes of bonds versus the membrane normal have been determined because SEIDAS monitors only those vibrations whose dipole moment are oriented perpendicular to the solid surface. The application of negative membrane potentials ($\Delta V = -0.3$ V) leads to the selective halt of the light-induced proton transfer at the stage of D75, the counter ion of the retinal Schiff base. It is inferred that the voltage raises the energy barrier of this particular proton-transfer reaction, rendering the energy deposited in the retinal by light excitation insufficient for charge transfer to occur. The other structural rearrangements that accompany light-induced activity of the membrane protein, are essentially unaffected by the transmembrane electric field. Our results demonstrate that SEIDAS is a generic approach to study processes that depend on the membrane potential, like those in voltage-gated ion channels and transporters, to elucidate the mechanism of ion transfer with unprecedented spatial sensitivity and temporal resolution.

ion transfer | membrane potential | proton translocation | vibrational spectroscopy | sensory rhodopsin

The transport and receptor function of membrane proteins is triggered by various external stimuli, e.g., light (as in the photosystems and the rhodopsins), electrons (as in the respiratory-chain complexes), ligands (as in G protein-coupled receptors, the cys-loop superfamily, and ATP activated cationic channels), or a change in membrane potential (as in voltage-gated ion channels). Because of their central role in cellular function, they are the target of 50% of all pharmaceutical drugs. Despite their biomedical relevance, molecular knowledge about the structure and function of these therapeutical targets is scant. The 3D structure of voltage-gated ion channels has been resolved in pioneering studies (1). However, it was the emerging patch-clamp technique that contributed, before the crystallographic studies, to the understanding of the action dynamics of ion channels (2). Although highly sensitive to electrical signals, patch clamp suffers from structural insensitivity and is, thus, unable to reveal mechanistic details on the atomic level. In contrast, IR spectroscopy is capable of discerning the structural changes associated with ion transfer (3). By recording differences between reaction states of the protein (4), alterations as minute as protonation reactions and modulations in H-bonding of single amino acid side chains or water molecules (5) are detected with time resolution as high as a few nanoseconds (6). Usually, stacks of membrane proteins have been necessary to achieve sufficient absorbance from >200 layers under attenuated total reflection conditions (7) (ATR, Fig. 1*A*), hindering IR spectroscopic studies that target the functionality of electron- or potential-triggered proteins. These obstacles were overcome by surface-enhanced IR spectroscopy (SEIRA) (Fig. 1*A*) where the presence of a rough surface of coinage metals leads to the 10- to 100-fold intensity enhancement of the vibrational bands of surface-adhered molecules (8).

The immobilization of proteins on the solid surface is achieved by a variety of different methodologies that exploit covalent or noncovalent interaction of the molecule with the surface (9). Proteins can be tethered chemoselectively via a genetically engineered His-tag to the Ni-NTA modified gold surface (10, 11). The use of affinity tags yields orientated protein molecules along the solid surface. Importantly, surface-adhered membrane proteins are reconstituted directly at the surface into a lipid bilayer by detergent removal (12, 13). The high surface sensitivity renders SEIRAS an exquisite method for studies of monolayers of surface-attached proteins. In combination with electrochemical methods, we have investigated proteins that participate in cellular redox chemistry. Structural changes of the protein induced by electron transfer from the solid electrode have been resolved on the level of single bonds (14, 15).

In this work, we have studied the influence of the electrical field on the reaction mechanism of sensory rhodopsin II (SRII) (16). SR II is the primary light sensor for the photophobic response of halobacteria (17). It is a member of the growing family of microbial rhodopsins that act as light-driven pumps, sensors, and channels (18). Some of these properties have recently been exploited in neurophysiological experiments to rapidly activate or silence neural circuits with light (19). The polypeptide of SR II folds into the membrane in the form of seven α-helices and harbors *all-trans* retinal as a chromophore that is covalently bound via a Schiff base linkage to a lysine residue of the apo-protein. The crystal structure of this membrane protein has been solved (20, 21) with the help of cubic phase crystallization (22), even in complex to its cognate transducer (23, 24). The high-resolution structure sets the basis for studies on the reaction mechanism.

In every living cell, ion pumps, channels, and transporters create and employ the energy of the membrane potential. It is evident that membrane proteins are influenced by the ubiquitous

Author contributions: F.S., K.A., R.V., and J.H. designed research; X.J., E.Z., M.S., K.A., and R.V. performed research; M.E. and R.S. contributed new reagents/analytic tools; X.J., E.Z., F.S., K.A., R.V., and J.H. analyzed data; and R.V. and J.H. wrote the paper.

The authors declare no conflict of interest.

This article is a PNAS Direct Submission. P.B. is a guest editor invited by the Editorial Board.

[†]X.J. and E.Z. contributed equally to this work.

[‖]To whom correspondence may be addressed. E-mail: joachim.heberle@uni-bielefeld.de or reiner.vogel@biophysik.uni-freiburg.de.

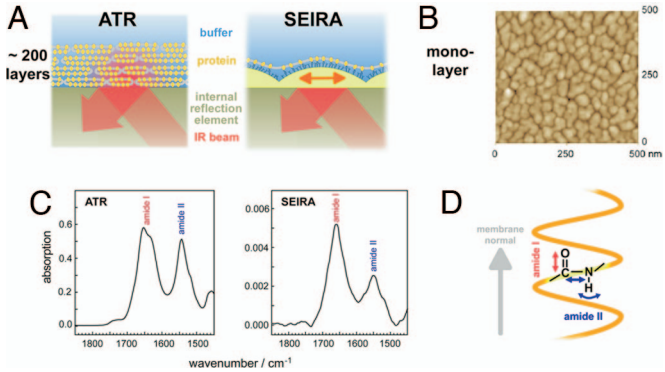

Fig. 1. Infrared spectroscopy on membrane proteins. (*A*) ATR spectroscopy probes stacks of several hundred membrane layers by the evanescent IR field atop an internal reflection element. The large number of membrane layers enables sufficiently high signal but hampers ligand binding or application of membrane potentials. In SEIRA spectroscopy, the IR field is enhanced by a nanostructured Ni-NTA modified gold film because of excitation of surface plasmons, allowing spectroscopic studies on a self-assembled membrane protein monolayer, selectively. (*B*) Atomic-force microscopic image of the rough gold surface used for SEIRA. The diameter of the gold nanoparticles is ≈50 nm with a height of 10 nm atop the continuous gold layer of 20 (±10) nm thickness. (*C*) ATR/FT-IR absorption spectra of a stack of the membrane protein sensory rhodopsin II reconstituted in halobacterial lipids (*Left*) in comparison with the SEIRA spectrum of a monolayer of SR II tethered to the modified gold surface via a His-tag (*Right*). The spectra have been corrected for vibrational contributions from the solvent water (scissoring mode of H_2O at ≈1,645 cm^{-1}). (*D*) Differing intensities of amide I and II vibrational modes of the protein backbone are due to their microscopic orientation and the polarization of the enhanced field with respect to the membrane normal.

potential difference across the cellular membrane in which they are embedded. Yet, it was impossible to elaborate the impact of the membrane potential on the functionality of a membrane protein, in general, and on specific steps of the reaction mechanism, in particular, because of experimental difficulties. We show here that SEIRAS provides the sensitivity to resolve the impact of the electrical field across the SR II monolayer on the level of atoms and bonds. Evidence is provided for the selective halt of proton transfer from the retinal Schiff base to the aspartic proton acceptor at potentials <-0.3 V. Alterations in the orientation of bonds that are associated with dipole moment changes perpendicular to the membrane surface are determined with acute sensitivity by surface-enhanced IR difference absorption spectroscopy (SEIDAS). Finally, our study demonstrates the generic character of SEIDAS as a methodology to be readily applicable to membrane proteins whose function is triggered by the membrane potential, like, e.g., that of voltage-gated ion channels.

Results and Discussion

SEIDAS on Sensory Rhodopsin II. Recombinant sensory rhodopsin II (25, 26) was specifically adhered via the C-terminal His-tag to the Ni-NTA modified gold surface. The latter was created a top the Si hemiprism used for internal reflection spectroscopy. The surface plasmon polariton generated at the rough gold surface (Fig. 1*B*) penetrates into the adjacent medium with a decay length of ≈8 nm sampling only those molecules that are within this short distance from the solid surface (8). Excitation of the surface plasmon by IR radiation leads to the enhancement of the vibrational bands from those chemical bonds whose orientation is perpendicular to the gold surface. Because of this surface selection rule, the SEIRA spectrum of SR II exhibits a strong amide I and a weak amide II band (Fig. 1*C Right*) as a consequence of the predominant perpendicular orientation of the transmembrane helices relative to the gold surface: The amide I mode of the α-helix is parallel to and the amide II mode is perpendicular to the helix axis and, thus, to the membrane normal (Fig. 1*D*). In contrast, the conventional ATR/FT-IR absorbance spectrum (Fig. 1*C Left*) shows a strong amide II band.

Light-Induced SEIDAS. Reaction-induced difference spectra were recorded to examine the vibrational changes of the dark versus the lit state of the SR II monolayer. Illumination of SR II from *N. pharaonis* (*N. p.*) with blue-green light creates a photostationary state that is probed by SEIDAS (Fig. 2*A*, black trace). The negative bands correspond to the vibrations of SR II in the dark state that are converted into positive bands in the long-lived intermediate state (M intermediate). Although the SEIDA spectrum is recorded from a single monolayer, the surface enhancement allows its detection with good signal-to-noise ratio. The SEIDA spectrum bears great similarity to the ATR difference spectrum recorded with polarized IR radiation when only those vibrations are monitored with dipole moment parallel to the membrane normal (*z* component, red trace). The comparison demonstrates that the selection rule of surface-enhanced

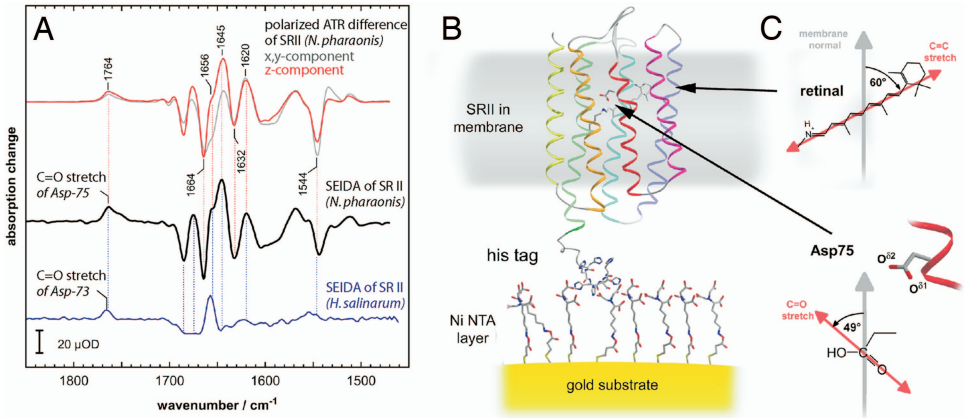

Fig. 2. SEIDA spectroscopy on a membrane protein. (*A*) Light-induced SEIDA spectra of sensory rhodopsin II from *N. p.* (black trace) and from *H. s.* (blue trace) reflect the transition from the resting dark state (negative bands) to the photoactivated state (positive bands). The *z*-component of the difference spectrum of *N. p. SR II* as determined by conventional ATR spectroscopy under polarized conditions (red trace), demonstrates that SEIDA selectively probes vibrations with dipole vectors parallel to the membrane normal. For comparison, the *x,y* component is also shown (gray trace), which corresponds to the in-plane orientation. (*B*) Structural model of sensory rhodopsin II bound via the C-terminal His-tag to the Ni-NTA modified gold surface (24). (*C*) Magnified structure and spatial orientation of the cofactor retinal and of the side chain of the proton acceptor D75 versus the membrane normal.

vibrational spectroscopy also holds for difference spectra. The most prominent difference bands of the SEIDA spectrum are categorized into bands of the cofactor retinal (1,500–1,600 cm^{-1}), amide I bands of the peptide bonds (1,620–1,680 cm^{-1}) that indicate structural changes of the protein backbone and bands of carboxylic acids and amide side chains (1,690–1,770 cm^{-1}). Specifically, the C═C stretching vibration of retinal absorbs at 1544 cm^{-1} (−) in ground-state SR II. The large angle of 60° with respect to the membrane normal renders the intensity of this band small. The negative band indicates deprotonation of the Schiff base (C═N-H in Fig. 2*C*) as a consequence of the *trans* to *cis* isomerization of retinal. The released proton is transferred to the acceptor D75 as deduced from the appearance of the C═O stretching vibration at 1,764 cm^{-1} reflecting the protonation of the carboxylate (27). The angle of the C═O bond of D75 to the membrane normal is determined to 49° (see *Materials and Methods*). By comparison with the 3D structure of the M state of SR II (24), we are able to univocally assign the band to the C═$O^{\delta 1}$ bond of the terminal carboxylic acid group of D75. Consequently, the Schiff base proton is transferred to the $O^{\delta 2}$ of the carboxylate. The charge redistribution within the protein is accompanied by structural changes of the protein backbone reflected by amide I difference bands at 1,620 (+), 1,632 (−), 1,645 (+), 1,656 (+), and 1,664 cm^{-1} (−). The surface selection rule magnifies the amide I changes because the structural changes occur in the helices that are oriented mostly parallel to the membrane normal.

Light-induced SEIDA spectroscopy was also conducted on SR II from *Halobacterium salinarum* (*H. s.*) to gauge the functional changes of the closely related protein. Indeed, *H. s.* SR II shows qualitatively similar vibrational features (blue trace in Fig. 2*A*) like the transient protonation of D73 (homologous residue to D75 of *N. p.* SRII). However, a very different signature is apparent in the amide I range. This observation reveals structural changes in *H. s.* SR II clearly distinct from those in the *N. p.* receptor (26). The absence of a negative band at 1,544 cm^{-1} indicates that the dipole moment of the C═C stretch of retinal is close to parallel to the solid surface. Again, the light-induced SEIDA spectrum of *H. s* SR II is identical to the *z*-polarized ATR difference spectrum (data not shown).

Impact of the Applied Electric Field. Most, if not all, biophysical techniques that are able to resolve structural changes on the atomic level, do not account for the membrane potential that is ubiquitous to living cells. With the gold substrate used for surface enhancement serving as the working electrode, light-induced SEIDA spectra have been recorded under different potentials versus the counter and reference electrodes (Fig. 3). Setting out from the open circuit potential (corresponding to 0.2 V, black trace) to more positive voltages, the light-induced SEIDA spectrum of SR II from *N. p.* is invariant toward the applied field.** In contrast, the decrease in potential gradually reduces the intensity of the band at 1,764 cm^{-1} until it almost completely disappears at a voltage of −0.3 V. The band at 1,764 cm^{-1} corresponds to the C═O stretching vibration (*vide supra*) and indicates proton transfer to D75, which is evidently blocked at the potential of −0.3 V. We conclude from this observation that the height of the energy barrier of the proton transfer reaction from the retinal Schiff base to D75 is increased at negative potentials. Evidently, the energy deposited in the retinal after light excitation is not sufficient to overcome the barrier raised by the voltage of −0.3 V. Thus, proton transfer to D75 cannot take place. This spectroscopic finding provides the

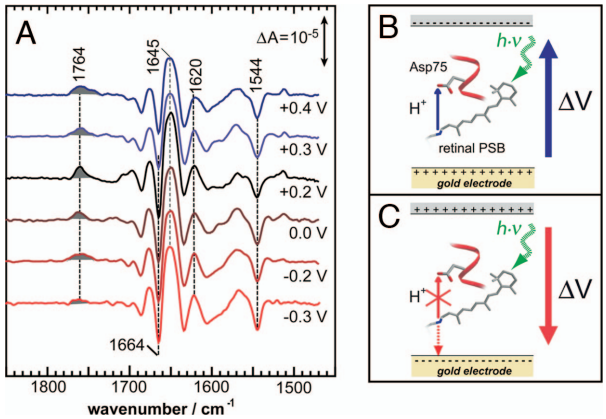

Fig. 3. SEIDA spectra at various transmembrane voltages across the membrane protein monolayer. (*A*) IR difference spectra of sensory rhodopsin II from *N. p.* were recorded at potentials from +0.4 V to −0.3 V (from top to bottom). Applied voltages are given versus the normal hydrogen electrode. (*B*) Sketch of the light-induced (green broken arrow) proton transfer reaction (thin blue arrow) from the donating retinal Schiff base of sensory rhodopsin II to the accepting carboxylic side chain of D75. The proton transfer step occurs in the same direction as the electric field vector (thick blue arrow that indicates the transmembrane voltage ΔV between the working gold electrode (+) and the counter electrode (−). (*C*) Protonation of D75 ceases (crossed out red upward arrow) when ΔV is opposite (bold red arrow) and lower than −0.2 V. In this case, the Schiff base proton is driven by the negative voltage toward the cytoplasmic side (red downward arrow).

molecular basis for the electrophysiological observation that the light-induced current is reduced with hyperpolarization (28). The voltage-dependent inhibition of the proton transfer is corroborated by experiments on SR II from *H. s.* (Fig. 4) but with the inhibition at somewhat less negative voltage as compared to SR II from *N. p.* Thus, we infer that the dependence of the functionality of SR II on the membrane potential varies among proteins of different origin.

The selective halt of proton transfer might be interpreted in terms of a field-induced shift in pK_a of the proton accepting D75 that achieves protonation of this residue even in the resting dark

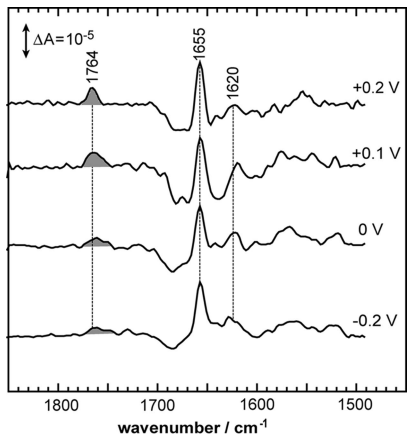

Fig. 4. Interspecies differences in the voltage-dependence of the light-induced SEIDA spectra of sensory rhodopsin II (SR II). The SEIDA spectra of SR II from *H. s.* show a similar voltage-induced halt of the light-induced proton transfer reaction from the protonated Schiff base to Asp-73 as observed in SR II from *N. p.* (Fig. 3). However, as manifested by the decreasing amplitude of the Asp-73 protonation band at 1,764 cm^{-1}, the halt occurs already at 0 V, indicating a species-dependent alteration of the energetics of this ion-transfer reaction. Experimental conditions are identical to the experiments on SR II from *N. p.*, but spectra were recorded across a narrower voltage range (Fig. 3).

**The spectral broadening of the band at 1764 cm^{-1} at high voltages is related to the influence of the electric field on the hydrogen-bonded network interacting with the C═O stretching vibration of D75.

state (29). However, such a protonation would lead to a substantial frequency shift of the ethylenic stretch of retinal at 1,544 cm^{-1}, which is not observed in our experiments. Thus, the electrical potential does not affect the protonation equilibrium of the acceptor group in the resting state but the light-dependent proton-transfer reaction itself. At negative potentials, the Schiff base proton dissociates and is driven by the electrical potential toward the cytoplasmic side, i.e., opposite to the physiological direction (Fig. 3*B*). However, vibrational bands of proton-accepting groups other than D75 could not be identified at the present signal-to-noise ratio of the SEIDA spectra. Alternatively, proton dissociation may be inhibited, keeping the Schiff base protonated in the photoactivated state. In this case, a positive contribution of retinal's ethylenic mode is expected, which might be contained in a shoulder at $\approx$1,570 cm^{-1}, indicating an N-type intermediate. Potential-dependent accumulation of a red-shifted (O-type) intermediate can be excluded by the absence of a band at 1,538 cm^{-1} (30).

In summary, the vibrational spectra are distinct markers for the molecular perturbation exerted by the electrical potential on the reaction mechanism of a transmembrane protein. The structural changes of the protein backbone as monitored by vibrational bands in the amide I region, are hardly affected by the applied potential. Consequently, the neutralization of charges by proton transfer from the Schiff base to D75 are not the cause for the structural changes in the helical protein backbone. This result agrees with experiments in which the D75N mutation leads to a photoreceptor that exhibits photoinduced changes in the amide I modes (31) and which is active in signal transfer to the cognate HtrII transducer (32). Thus, we conclude that it is the transient proton transfer from the retinal Schiff base to D75 that is sensitive to the electrical potential rather than the pH-dependent equilibrium of a protonatable residue (29).

Conclusions

The presented SEIDA data complement those derived from surface-enhanced resonance Raman spectroscopy (SERRS) that reveal distinct structural changes of the retinal cofactor dependent on the applied potential (33). Thus, spectroscopic methods that combine structural and electrochemical sensitivity are highly relevant and form the basis of the biophysical scrutiny of the physiological function of membrane proteins and its regulation by the membrane potential. Electrochemical triggering via a solid electrode also opens an avenue to investigations of electron-driven systems, such as the membrane protein (super-) complexes of the respiratory chain and the photosynthetic apparatus, because electrons can be directly injected from the electrode into the protein. Of equal biomedical relevance are voltage-gated ion channels whose functional mechanism can be addressed on the level of individual vibrations by SEIDA spectroscopy under voltage-clamp conditions. The reaction dynamics will ultimately be provided by time-resolved SEIDA spectroscopy, performed by integrating the step-scan technique (3, 6) with SEIDA. In fact, we recently succeeded in monitoring structural changes associated with electron injection into a monolayer of cytochrome *c* with a time resolution of 65 μs (K.A. and J.H., unpublished work). As the methodology is readily applicable to membrane proteins, SEIDA is poised to reveal mechanistic insights into this important class of proteins to follow ion translocation with high spatiotemporal resolution.

Materials and Methods

The rough gold surface used for SEIRA spectroscopy was modified by nickel chelating nitrilo-triacetic acid (Ni-NTA) according to published procedures (12, 14, 34). Each modification step was followed *in situ* by SEIRAS. His-tagged sensory rhodopsin II (SR II) from *N. p.* and from *H. s.* were expressed and purified as described (25, 26). Binding of SR II via the C-terminal His-tag to the Ni-NTA modified gold surface was carried out by incubating a 6 μM solution of protein in 0.05% (wt/vol) *n*-dodecyl-β-D-maltopyranoside (DDM) (pH 5.8, 20°C, 4 M NaCl, 50 mM phosphate buffer, in the case of SRII from *H. s.*) or a 4.0 μM solution of protein in 0.02% DDM (pH 8.0, 20°C, 0.5M NaCl, 10 mM bis-Tris-propane buffer, in the case of SRII from *N. p.*) atop the Ni-NTA modified gold surface. Reconstitution of the membrane protein in the lipid bilayer by detergent removal (12) and the parallel addition of polar lipids from the purple membrane of *H. s.* (35) or phosphatidylcholine from egg yolk (Sigma) at a protein/lipid ratio of 1:20 stabilized the protein to achieve a good signal-to-noise ratio in the IR difference spectra by extensive signal averaging (*vide infra*). Saturation of protein binding to the modified surface occurred within $\approx$1.5 h. For light-induced IR difference spectroscopy, the protein was excited through a fiber optic by light from a 150 W tungsten lamp filtered by a narrow band filter (480–505 nm) in the case of SRII from *N. p.* or by a light-emitting diode (LED; Luxeon Star) with the emission maximum at 497 nm (23 nm FWHM) and an intensity of 10 mW/cm^2 in the case of SRII from *H. s.*

IR spectra were recorded in Freiburg on an IFS 28 or in Bielefeld on an IFS 66v/S spectrometer (Bruker). SEIRA spectroscopy was conducted with home-built single reflection units using hemicylindrical Si internal reflection elements (12, 14, 15). To achieve a noise level that allows for the detection of absorbance bands as weak as 10^{-6}, typically 1,024 scans were coadded at a spectral resolution of 4 cm^{-1} and $\approx$70 of such spectra were averaged. Attenuated total reflection IR spectroscopy of the membrane protein immersed in 4 M NaCl was performed with a microATR accessory (Resultec) that uses a diamond reflection element with six effective reflections (7). Polarized ATR spectra were recorded by using a custom-made ATR unit with a Ge internal reflection element with seven effective reflections and KRS-5 12.000 grid polarizers (Graseby Specac). Light-induced ATR difference spectra were recorded with polarizer settings parallel and perpendicular to the plane of incidence from hydrated films of SR II reconstituted into purple membrane lipids at a 1:30 molar ratio. These spectra were converted into their *z*- and *x*,*y*-components polarized perpendicular and parallel, respectively, to the surface of the internal reflection element by using the Harrick thick-film formalism (35), which was warranted by the film conditions.

Voltages across the surface-adhered protein monolayer were applied between the gold surface and a platinum mesh. The potential reference was a Ag/AgCl electrode which finally established the three-electrode system running in the potentiostatic mode (12, 14). Voltages given are versus the normal hydrogen electrode ($\Delta E_{NHE} = \Delta E_{Ag/AgCl} + 0.2$ V). It is noted that the given voltages are those applied to the electrodes. The resulting electric field strength that drops off the membrane cannot be quantitatively assessed because of the unknown dielectric properties of the solid-supported membrane. Yet, we assume that the potential drop is across the Stern layer where the solid-supported membrane is located.

ACKNOWLEDGMENTS. We thank Rebecca M. Nyquist for reading the manuscript; R.S. thanks Georg Büldt for generous support; and J.H. acknowledges helpful discussions with Eberhard Neumann and Benjamin Kaupp. This work was supported by grants from the German Ministry for Science and Education (to J.H.) and Deutsche Forschungsgemeinschaft Grant Vo 811/3,4 (to R.V.) and Za 566/1-1 (to E.Z.). X.J. thanks the Alexander-von-Humboldt foundation for a fellowship.

1. Gouaux E, MacKinnon R (2005) Principles of selective ion transport in channels and pumps. *Science* 310:1461–1465.
2. Sakmann B, Neher E (1984) Patch clamp techniques for studying ionic channels in excitable membranes. *Annu Rev Physiol* 46:455–472.
3. Garczarek F, Gerwert K (2006) Functional waters in intraprotein proton transfer monitored by FTIR difference spectroscopy. *Nature* 439:109–112.
4. Mäntele W (1993) Reaction-induced infrared difference spectroscopy for the study of protein function and reaction mechanisms. *Trends Biochem Sci* 18:197–202.
5. Kandori H, Furutani Y, Shimono K, Shichida Y, Kamo N (2001) Internal water molecules of pharaonis phoborhodopsin studied by low-temperature infrared spectroscopy. *Biochemistry* 40:15693–15698.
6. Rödig C, Chizhov I, Weidlich O, Siebert F (1999) Time-resolved step-scan Fourier transform infrared spectroscopy reveals differences between early and late M intermediates of bacteriorhodopsin. *Biophys J* 76:2687–2701.
7. Nyquist RM, Ataka K, Heberle J (2004) The molecular mechanism of membrane proteins probed by evanescent infrared waves. *Chembiochem* 5:431–436.
8. Osawa M (2002) in *Handbook of Vibrational Spectroscopy*, eds Chalmers JM, Griffiths PR (Wiley, Chichester, UK), pp 785–799.
9. Camarero JA (2008) Recent developments in the site-specific immobilization of proteins onto solid supports. *Biopolymers* 90:450–458.
10. Sigal GB, Bamdad C, Barberis A, Strominger J, Whitesides GM (1996) A self-assembled monolayer for the binding and study of histidine tagged proteins by surface plasmon resonance. *Anal Chem* 68:490–497.

11. Dietrich C, Schmitt L, Tampe R (1995) Molecular organization of histidine-tagged biomolecules at self-assembled lipid interfaces using a novel class of chelator lipids. *Proc Natl Acad Sci USA* 92:9014–9018.
12. Ataka K, *et al.* (2004) Oriented attachment and membrane reconstitution of His-tagged cytochrome *c* oxidase to a gold electrode: *In situ* monitoring by surface-enhanced infrared absorption spectroscopy. *J Am Chem Soc* 126:16199–16206.
13. Ataka K, Richter B, Heberle J (2006) Orientational control of the physiological reaction of cytochrome *c* oxidase tethered to a gold electrode. *J Phys Chem B* 110:9339–9347.
14. Ataka K, Heberle J (2007) Biochemical applications of surface-enhanced infrared absorption spectroscopy. *Anal Bioanal Chem* 388:47–54.
15. Ataka K, Heberle J (2003) Electrochemically induced surface-enhanced infrared difference absorption (SEIDA) spectroscopy of a protein monolayer. *J Am Chem Soc* 125:4986–4987.
16. Hoff WD, Jung KH, Spudich JL (1997) Molecular mechanism of photosignaling by archaeal sensory rhodopsins. *Annu Rev Biophys Biomol Struct* 26:223–258.
17. Hildebrand E, Dencher N (1975) Two photosystems controlling behavioural responses of *Halobacterium halobium*. *Nature* 257:46–48.
18. Klare JP, Chizhov I, Engelhard M (2008) Microbial rhodopsins: Scaffolds for ion pumps, channels, and sensors. *Results Probl Cell Differ* 45:73–122.
19. Zhang F, *et al.* (2007) Multimodal fast optical interrogation of neural circuitry. *Nature* 446:633–639.
20. Luecke H, Schobert B, Lanyi JK, Spudich EN, Spudich JL (2001) Crystal structure of sensory rhodopsin II at 2.4 Å: Insights into color tuning and transducer interaction. *Science* 293:1499–1503.
21. Royant A, *et al.* (2001) X-ray structure of sensory rhodopsin II at 2.1- Å resolution. *Proc Natl Acad Sci USA* 98:10131–10136.
22. Landau EM, Rosenbusch JP (1996) Lipidic cubic phases: A novel concept for the crystallization of membrane proteins. *Proc Natl Acad Sci USA* 93:14532–14535.
23. Gordeliy VI, *et al.* (2002) Molecular basis of transmembrane signalling by sensory rhodopsin II-transducer complex. *Nature* 419:484–487.
24. Moukhametzianov R, *et al.* VI (2006) Development of the signal in sensory rhodopsin and its transfer to the cognate transducer. *Nature* 440:115–119.
25. Hohenfeld IP, Wegener AA, Engelhard M (1999) Purification of histidine tagged bacteriorhodopsin, pharaonis halorhodopsin and pharaonis sensory rhodopsin II functionally expressed in *Escherichia coli*. *FEBS Lett* 442:198–202.
26. Mironova OS, *et al.* (2005) Functional characterization of sensory rhodopsin II from *Halobacterium salinarum* expressed in *Escherichia coli*. *FEBS Lett* 579:3147–3151.
27. Engelhard M, Scharf B, Siebert F (1996) Protonation changes during the photocycle of sensory rhodopsin II from *Natronobacterium pharaonis*. *FEBS Lett* 395:195–198.
28. Schmies G, Engelhard M, Wood PG, Nagel G, Bamberg E (2001) Electrophysiological characterization of specific interactions between bacterial sensory rhodopsins and their transducers. *Proc Natl Acad Sci USA* 98:1555–1559.
29. Bombarda E, Becker T, Ullmann GM (2006) Influence of the membrane potential on the protonation of bacteriorhodopsin: Insights from electrostatic calculations into the regulation of proton pumping. *J Am Chem Soc* 128:12129–12139.
30. Furutani Y, *et al.* (2004) FTIR Spectroscopy of the O photointermediate in pharaonis phoborhodopsin. *Biochemistry* 43:5204–5212.
31. Hein M, Radu I, Klare JP, Engelhard M, Siebert F (2004) Consequences of counterion mutation in sensory rhodopsin II of *Natronobacterium pharaonis* for photoreaction and receptor activation: An FTIR study. *Biochemistry* 43:995–1002.
32. Inoue K, Sasaki J, Spudich JL, Terazima M (2007) Laser-induced transient grating analysis of dynamics of interaction between sensory rhodopsin II D75N and the HtrII transducer. *Biophys J* 92:2028–2040.
33. Rivas L, Hippler-Mreyen S, Engelhard M, Hildebrandt P (2003) Electric-field dependent decays of two spectroscopically different M-states of photosensory rhodopsin II from *Natronobacterium pharaonis*. *Biophys J* 84:3864–3873.
34. Ataka K, Heberle J (2006) Use of surface enhanced infrared absorption spectroscopy (SEIRA) to probe the functionality of a protein monolayer. *Biopolymers* 82:415–419.
35. Harrick, N. J (1967) *Internal Reflection Spectroscopy* (Wiley, New York).